Clin Rheumatol (2009) 28:271–276
DOI 10.1007/s10067-008-1034-6

ORIGINAL ARTICLE

Calcium pyrophosphate dihydrate crystal deposition disease: sonographic findings

A. Ciapetti · E. Filippucci · M. Gutierrez · W. Grassi

Received: 18 July 2008 / Revised: 5 October 2008 / Accepted: 22 October 2008 / Published online: 13 November 2008

Abstract High-resolution sonography is a rapidly evolving technique that is gaining an increasing success in the assessment of crystalline arthropathies. In calcium pyrophosphate dihydrate crystal deposition disease, the sonographic features of crystal deposition include hyperchoic spots within hyaline cartilage and/or fibrocartilage and soft tissue calcifications. The aim of this pictorial essay was to present the main findings evocative of crystal deposition in patients with pyrophosphate arthropathy.

Keywords Calcium pyrophosphate dihydrate crystal deposition disease · Cartilage · Tendons · Ultrasonography

Introduction

Calcium pyrophosphate dihydrate (CPPD) crystal deposition disease is characterized by acute or chronic inflammation due to deposit of CPPD crystals in articular cartilage and periarticular soft tissues [1, 2]. Over the last few years, the availability of high resolution probes in the field of musculoskeletal ultrasonography (US) has enabled the accurate detection of even minimal soft tissue abnormalities [3–6].

A. Ciapetti · E. Filippucci · M. Gutierrez · W. Grassi
Cattedra di Reumatologia, Università Politecnica delle Marche, Jesi, Ancona, Italy

E. Filippucci (✉)
Clinica Reumatologica, Università Politecnica delle Marche, Ospedale "A. Murri", Via dei Colli, 52, 60035 Jesi, Ancona, Italy
e-mail: emilio_filippucci@yahoo.it

With respect to the other imaging techniques, US has revealed great potential in the assessment of and soft tissue involvement in patient with CPPD crystal deposition disease [7–14]. Aggregates of CPPD crystals have a high reflectivity detectable in hyaline cartilage, fibrocartilage, synovial fluid, and various soft tissues such as ligaments and tendons. The aim of this pictorial was to present the principal US findings in patients with CPPD crystal deposition disease.

Materials and methods

The US pictures illustrated in this paper were obtained in a cohort of 42 consecutive patients with CPPD disease, with a diagnosis confirmed by synovial fluid analysis. The US examinations were performed using the following high-quality US systems: Diasus (Dynamic Imaging, Livingstone, UK, with an 8- to 16-MHz linear probe), Logiq 9 (General Electric Medical Systems, with an 8- to 15-MHz linear probe), and MyLab70 (Esaote Biomedica, Genoa, Italy, with a 6- to 18-MHz linear probe). The US scans were performed at anatomic regions referred by patients as painful.

Results

Hyaline cartilage

The high spatial resolution of US (<0.1 mm) and the sparkling reflectivity of CPPD crystal aggregates allow the clear depiction of even very small hyperchoic spots (less than 1 mm in size) within hyaline cartilage. Typical CPPD crystal deposits can be seen within the substance of the

hyaline cartilage in different anatomical sites, including femoral condyle (Fig. 1) and metacarpal heads (Fig. 2). When the US beam encounters even minimal crystal aggregates, relative echoes are well visible even at very low levels of gain. Intra-articular CPPD crystal aggregates show a high variability with regard to the evolution phase of the disease. The range of possible expressions goes from isolated hyperchoic spot to extended deposits which may involve a wide portion of the hyaline cartilage (Fig. 3). Linear CPPD crystal deposits do not have a sufficient compactness to stop the US beam progression, enabling the visualization of the underline cortical bone profile. This is more relevant at level of hyaline cartilage of femoral condyle.

Usually, there is a close correlation between the appearance of crystal deposits on radiograph and on US. Sometimes, even minimal deposits of CPPD crystals can be detected by US when the radiograph is apparently normal [15] (Fig. 4).

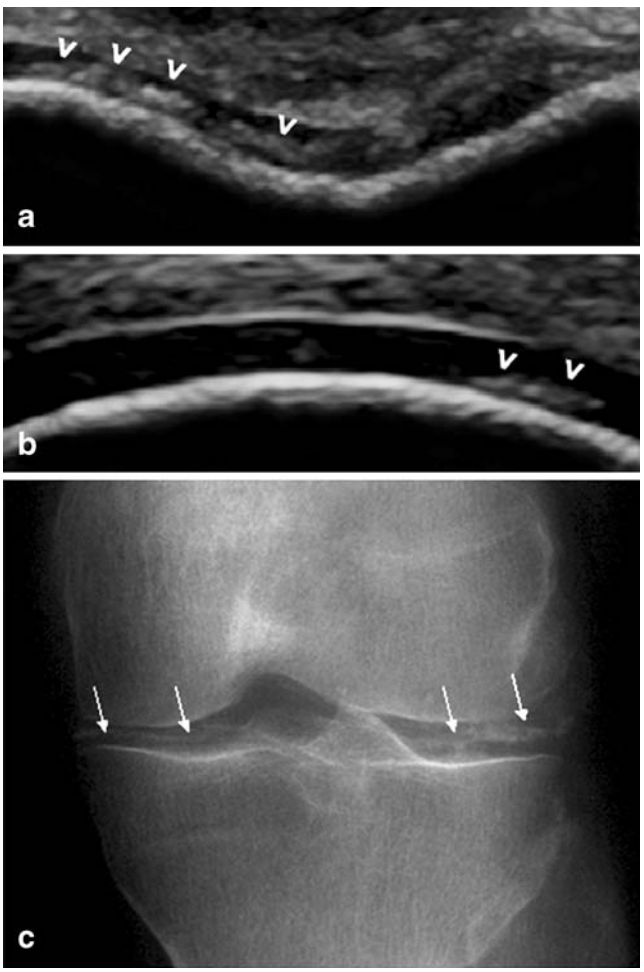

Fig. 1 Knee. **a**, **b** US on both transverse (**a**) and longitudinal (**b**) scans of the suprapatellar bursa show hyperechoic band within the femoral articular cartilage (*arrowheads*), not generating acoustic shadow. **c** Corresponding conventional radiography of hyaline and fibrocartilage calcification (*arrows*)

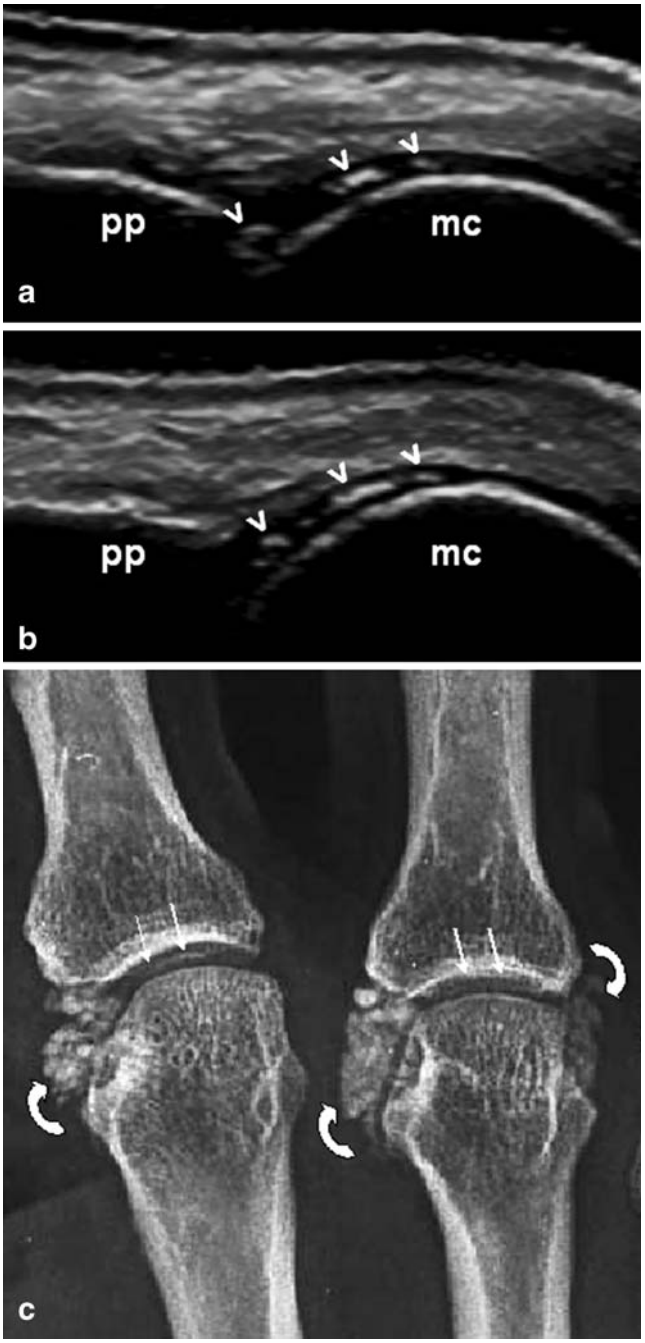

Fig. 2 Hand. **a**, **b** US on longitudinal scans shows hyperchoic deposits (*arrowheads*) within the substance of the articular cartilage of the metacarpal heads (*mc*) of the second and third finger. **c** Corresponding conventional radiography reveal calcification of the articular cartilage (*arrows*) and of the periarticular soft tissues (*curved arrows*). *pp* proximal phalanx

Fibrocartilage

US can show the presence of CPPD deposits within the fibrocartilage. These aggregates appear as hyperechoic rounded or amorphous-shaped areas and their location can be confirmed by dynamic assessment of the joint during

real-time scanning. The lack of adequate acoustic windows does not allow the proper US identification of CPPD crystals in all anatomic areas. CPPD aggregates can be easily identified by US in the menisci of the knee (Fig. 5) and in the triangular ligament of the wrist (Fig. 6).

Synovial fluid

US allows to detect echogenic aggregates floating in the synovial fluid. These aggregates, typically, are uniformly rounded in shape with sharply defined margins. Crystal aggregates should be distinguished from joint debris and proteinaceous material by demonstrating the reflectivity of the crystals present by adjustment of the US setting to a low level of power and gain (Fig. 7).

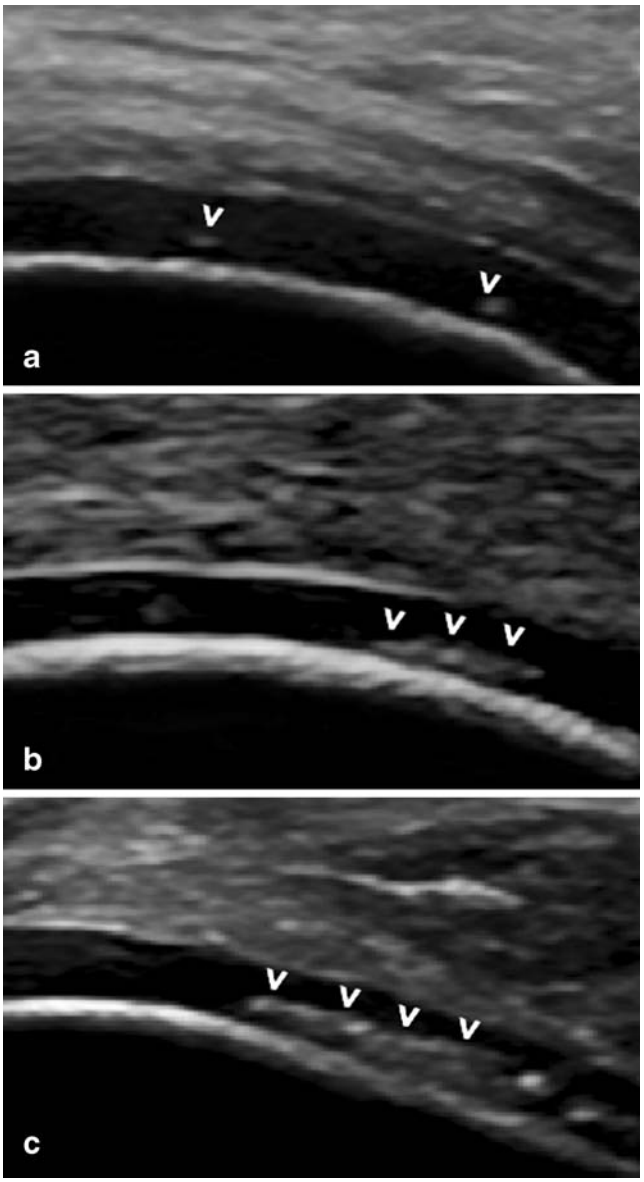

Fig. 3 Knee. Femoral condyle. Different pattern of focal hyperechoic deposits within the cartilage layer (*arrowheads*) not generating a posterior acoustic shadow: from small punctate aggregates (**a**) to larger solid deposits (**b**, **c**)

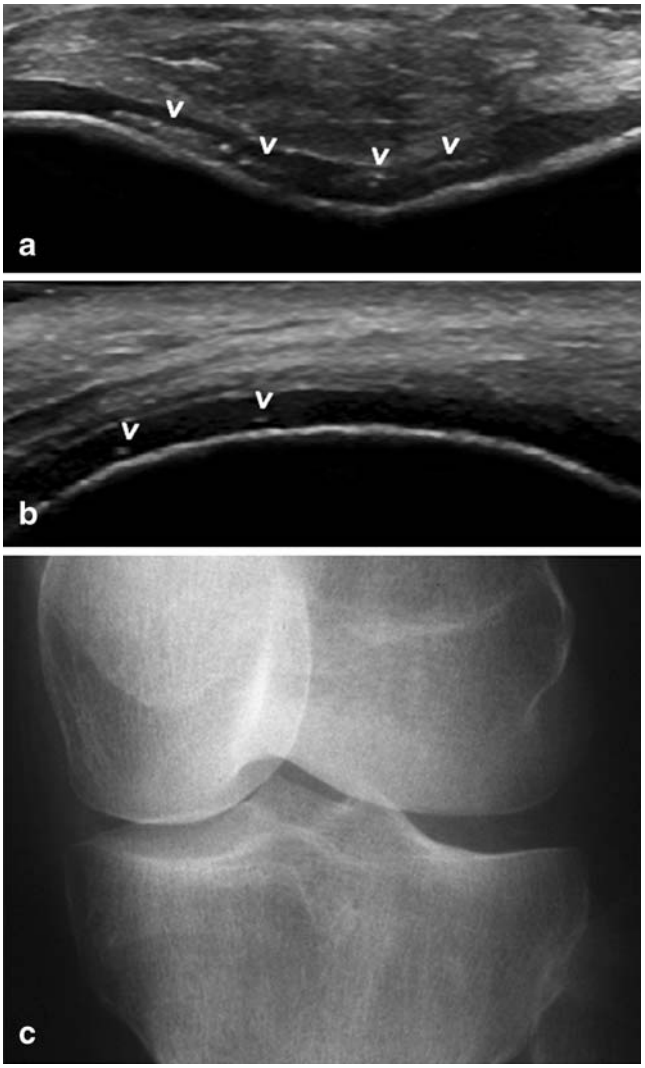

Fig. 4 Knee. **a**, **b** US on both transverse (**a**) and longitudinal (**b**) suprapatellar scans show hyperechoic areas within the hyaline cartilage of the femoral condyle (*arrowheads*) not detectable on conventional radiography (**c**)

Extra-articular soft tissues

CPPD crystal deposits of extra-articular soft tissues can be revealed by US examination. US is able to define the extension of crystal deposits and differentiate between intratendinous and paratendinous calcifications. CPPD crystal deposits may show a varying degree of shape and can generate acoustic shadow (Fig. 8). The deposition of CPPD crystals in tendons, for example, can be variable, depending on the position and the size of the aggregates. Intratendinous crystal deposits appear as hyperechoic spots or bands within the contest of the fibrillar echotexture of

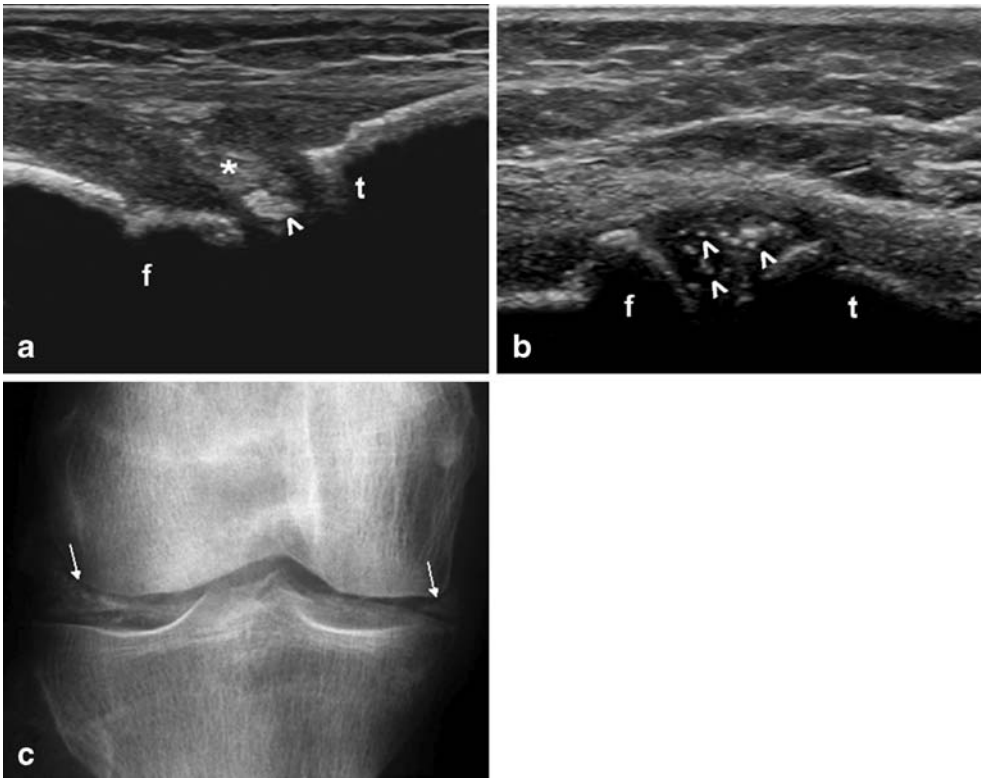

Fig. 5 Knee. US on lateral (**a**) and medial (**b**) longitudinal scans shows hyperechoic areas (*arrowheads*) within the fibrocartilage (*asterisk*). Of note the spectrum of US appearance of pyrophosphate crystal aggregates: from sharply defined hyperechoic ovoidal areas (**a**) to homogeneously punctate pattern (**b**). Corresponding conventional radiography (**c**) detects calcification of menisci (*arrows*). *f* femur, *t* tibia

tendons. Calcification of tendons in CPPD crystal deposition disease is typically linear and extensive and may generate an acoustic shadow (Fig. 9).

Discussion

This pictorial essay documents, according to the literature [7–9, 13, 14], that pyrophosphate crystal aggregates can be clearly depicted by US at different anatomical areas and tissues. US is a very promising tool to aid diagnosis of CPPD crystal deposition disease particularly in the setting of acute inflammatory arthritis, especially when other imaging modalities (such as conventional radiography) may be negative. The diagnostic role of US in cases of CPPD disease is "clearly" increased by the successful rate in the aspiration especially when very small amount of fluid are detected [16].

Sonographic features of CPPD deposits depend on the amount and distribution of aggregates of crystals. The spectrum of US appearance of CPPD crystal aggregates can vary from homogeneously punctate (within the contest of articular cartilage or floating in synovial fluid) to sharply defined hyperechoic band of variable size. The shape and anatomical location of the crystal aggregates in CPPD are extremely helpful to distinguish them from other crystal arthropathies. Differently from CPPD crystals, sodium

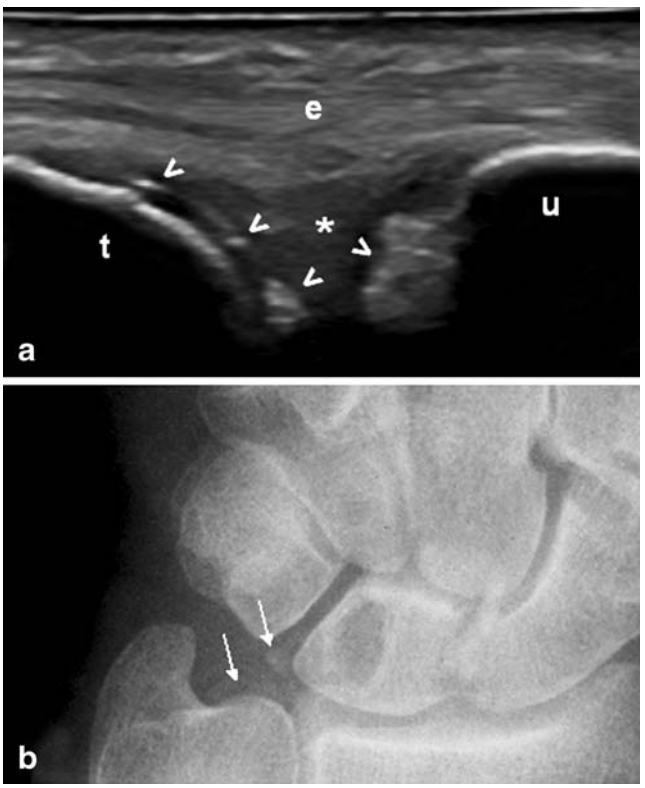

Fig. 6 Wrist. **a** Lateral longitudinal view shows hyperechoic areas (*arrowheads*) within the triangular ligament (*asterisk*). Calcifications of the triangular ligament (*arrows*) were detectable also on conventional radiography (**b**). *e* extensor carpi ulnaris tendon, *u* ulna, *t* triquetrum bone

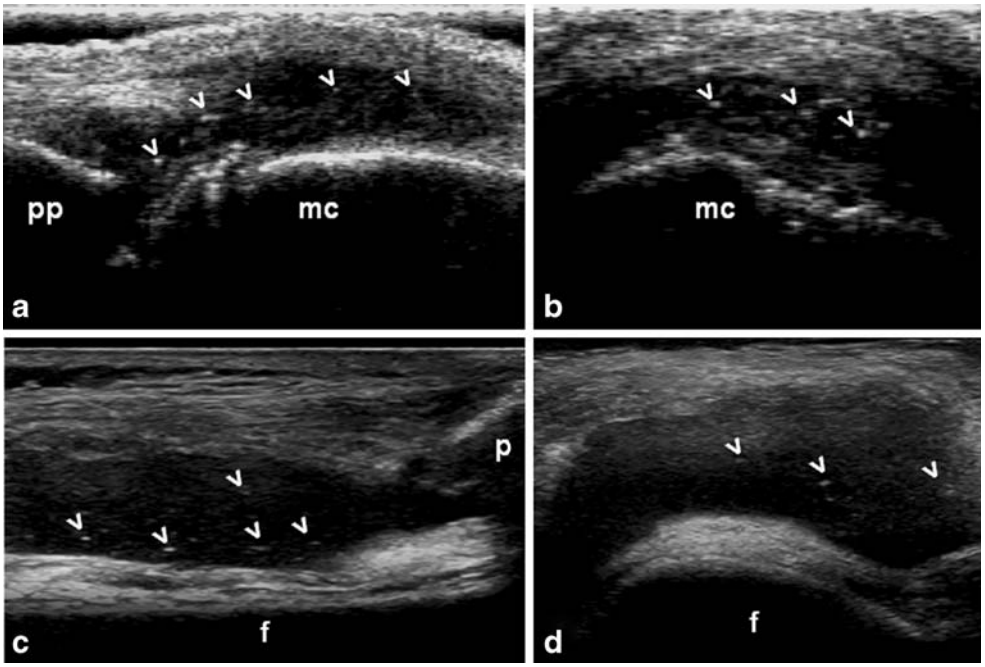

Fig. 7 Hand (**a**, **b**) and knee (**c**, **d**) in two patients with CPPD crystal deposition disease. Longitudinal (**a**, **c**) and transverse (**b**, **d**) scans show US findings indicative of synovitis of both metacarpophalangeal and knee joints. Hyperchoic punctate rounded aggregates appear as hyperechoic spots (*arrowheads*) floating in the contest of a mainly anechoic synovial fluid. *pp* proximal phalanx, *mc* metacarpal bone, *f* femur

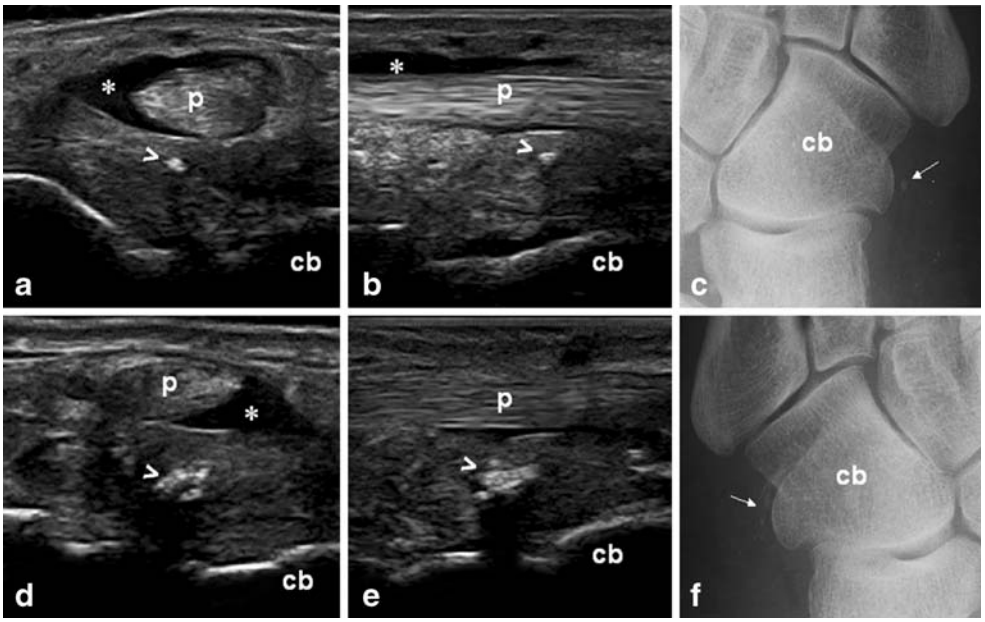

Fig. 8 Right (**a**–**c**) and left (**d**–**f**) foot. The transverse (**a**, **d**) and longitudinal (**b**, **e**) US scans of the peroneus longus tendon (*p*) of both sides in a subject with CPPD crystal deposition disease reveal, at level of cuboid bone (*cb*), the presence of hyperechoic areas (*arrowheads*) with posterior acoustic shadows. Of note bilateral anechoic tendon sheath widening of peroneus longus tendon (*asterisk*) indicative of essudative tenosynovitis. Calcifications were also detectable on conventional radiography (*arrows*) of the right (**c**) and left (**f**) foot

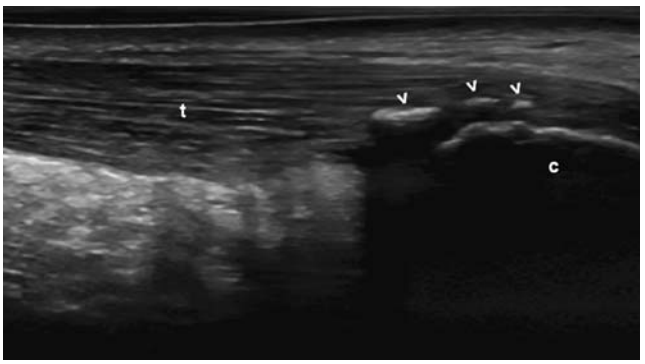

Fig. 9 Achilles tendon (*t*). The longitudinal scan shows intratendinous hyperchoic areas with acoustic shadows (*arrowheads*). *c* calcaneal bone ▶

monourate crystals deposits, for example, are not visualized within the hyaline cartilage.

Typically, urate deposits enhance the visualization of the superficial margin of the hyaline cartilage, increasing both its reflectivity and thickness. Despite US is not considered the gold standard imaging technique used for the diagnosis of CPPD crystals deposits disease, the direct visualization of these deposits allows the rheumatologist to gain a clearer interpretation of the meaning of the different clinical findings and may play a relevant role in disease diagnosis especially in case of synovitis and/or pain of uncertain origin.

Disclosures None

References

1. Resnick D, Niwayama G, Goergen TG, Utsinger PD et al (1977) Clinical, radiographic, and pathologic abnormalities in calcium pyrophosphate dihydrate deposition disease (CPPD): pseudogout. Radiology 122:1–15
2. Rothschild BM (1993) Identification of calcium pyrophosphate dihydrate crystals. Clin Exp Rheumatol 11:216–217
3. Kane D, Grassi W, Sturrock R, Balint PV (2004) Musculoskeletal ultrasound—a state of the art review in rheumatology. Part 2: clinical indications for musculoskeletal ultrasound in rheumatology. Rheumatology 43:829–838
4. Gibbon WW (2004) Applications of ultrasound in arthritis. Semin Musculoskelet Radiol 8:313–328
5. Grassi W, Salaffi F, Filippucci E (2005) Ultrasound in rheumatology. Best Pract Res Clin Rheumatol 19:467–485
6. Thiele RG, Schlesinger N (2007) Diagnosis of gout by ultrasound. Rheumatology 46:1116–1121
7. Grassi W, Meenagh G, Pascual E, Filippucci E (2006) "Crystal clear"—sonographic assessment of gout and calcium pyrophosphate deposition disease. Semin Arthritis Rheum 36:197–202
8. Sofka CM, Adler RS, Cordasco FA (2002) Ultrasound diagnosis of chondrocalcinosis in the knee. Skeletal Radiol 31:43–45
9. Foldes K (2002) Knee chondrocalcinosis: an ultrasonographic study of the hyalin cartilage. Clin Imaging 26:194–196
10. Coari G, Iagnocco A, Zoppini A (1995) Chondrocalcinosis: sonographic study of the knee. Clin Rheumatol 14:511–514
11. Delle Sedie A, Riente L, Iagnocco A, Filippucci E et al (2007) Ultrasound imaging for the rheumatologist X. Ultrasound imaging in crystal-related arthropathies. Clin Exp Rheumatol 25:513–517
12. Choi MH, MacKenzie JD, Dalinka MK (2006) Imaging features of crystal-induced arthropathy. Rheum Dis North Am 32:427–446
13. Frediani B, Filippou G, Falsetti P, Lorenzini S et al (2005) Diagnosis of calcium pyrophosphate dihydrate crystal deposition disease: ultrasonographic criteria proposed. Ann Rheum Dis 64:638–640
14. Filippou G, Frediani B, Gallo A, Menza L et al (2007) A "new" technique for the diagnosis of chondrocalcinosis of the knee: sensitivity and specificity of high-frequency ultrasonography. Ann Rheum Dis 66:1126–1128
15. Filippucci E, Gutierrez M, Georgescu D, Salaffi et al (2008) Hyaline cartilage involvement in patients with gout and calcium pyrophosphate deposition disease. An ultrasound study. Osteoarthr Cartil. doi:10.1016/j.joca.2008.06.003
16. Balint PV, Kane D, Hunter J, McInnes IB et al (2002) Ultrasound guided versus conventional joint and soft tissue fluid aspiration in rheumatology practice: a pilot study. J Rheumatol 29:2209–2213